HETEROCYCLES, Vol. 105, No. 1, 2022, pp. 477 - 486. © 2022 The Japan Institute of Heterocyclic Chemistry
Received, 15th March, 2022, Accepted, 25th April, 2022, Published online, 9th May, 2022
DOI: 10.3987/COM-22-S(R)19

N-HETEROCYCLIC ANALOGS OF INDENOCORANNULENE

Ansu Li,[1] Jun Xu,[1] Kim K. Baldridge,[1] and Jay S. Siegel[1]*

[1] School of Pharmaceutical Science and Technology, Tianjin University, 92 Weijin Road, Nankai District, Tianjin, 300072, China.

Abstract – Four chiral N-heterocyclic monoindenocorannulenes were prepared by fusing pyridine, quinoline, and indole across the *peri*-positions of corannulene via tandem Suzuki-aryl-aryl coupling and C-Cl activated ring closure reactions. The UV-Vis, fluorescence, and CV properties of these N-doped polynuclear aromatics are discussed. Resolution of enantiomers is performed on chiral stationary phase HPLC and the absolute configurations are assigned by comparison of experimental and quantum mechanically predicted ECD spectra.

INTRODUCTION

N-Heterocyclic aromatics are widely distributed in biomolecules and pharmaceutics.[1] Pyridine is a key component of soluble coenzymes, aiding in biological processes.[2] Quinoline and indole are versatile in medicinal chemistry, as they are components of a large number of pharmaceutically active molecules.[3-7] From the perspective of Lipinski, nitrogen atoms serve multiple purposes including increasing water solubility, adding alkaline functionality, and increasing hydrogen bond accepting capacity.[8] Pyridine and indole are considered as bioisosteric replacements for phenol group.[9] In contrast, polynuclear aromatic hydrocarbons (PAHs) are characteristically sparingly soluble in water, weak bases, and poor hydrogen bond acceptors. N-Doping polynuclear aromatic hydrocarbons with heteroatoms offer a wealth of molecular designs with tailored physical properties. Curved aromatic hydrocarbons with embedded nitrogen atoms are few, but pioneering examples can be found in nitrogen-embedded corannulene derivatives prepared from penta-aryl pyrroles,[10-14] as well as nitrogen and sulfur rim-doped bowl-shaped aromatics.[15-18] More recently, corannulene derivatives fused with pyridine and thiophene have been investigated with a focus on chiral modification and photo/electro-physical tuning.[19,20] This study highlights methods toward the hybridization of canonical N-aromatic heterocycles like pyridine, quinoline, and indole with corannulene to form a new set of chiral resolvable lead N-doped PAHs, the assignment of their configuration, and the characterization of their electrochemical and luminescent properties.

RESULTS AND DISCUSSION

Molecular Design and Synthesis

The origins of these molecular designs come from previous work on hybridizing planar and curved PAHs. Here the hybridization partners are corannulene and a subset of canonical N-heterocyclic aromatics (pyridine, quinoline, and indole). This design is exemplary but not exclusive or by any measure privileged. Specifically, fusion across the *peri*-position of corannulene (*indeno* fashion) affords a plausible modular chemical synthesis (Figure 1a), as well as good precedence that the fusion will impart structural rigidity toward bowl-inversion on the laboratory time scale.[21] Desymmetrization with functional groups or heteroatoms renders the bowl-conformers chiral and slowing the rate of inversion makes resolution and configurational stability a practical goal, as seen in the case of rim-substituted X-indenocorannulenes[22] (Figure 1b) and *sym*-pentaindenocorannulene derivatives (Figure 1c).[23] In addition, molecules hybridized by corannulene and helicene were designed and synthesized, whose chirality was derived from both bowl inversion and fused helical parts.[24] Recognizing these chiral indeno derivatives do not conform to CIP nomenclature; the specific configurational descriptor (乒 and 乓), established and reported previously, is applied here.[22]

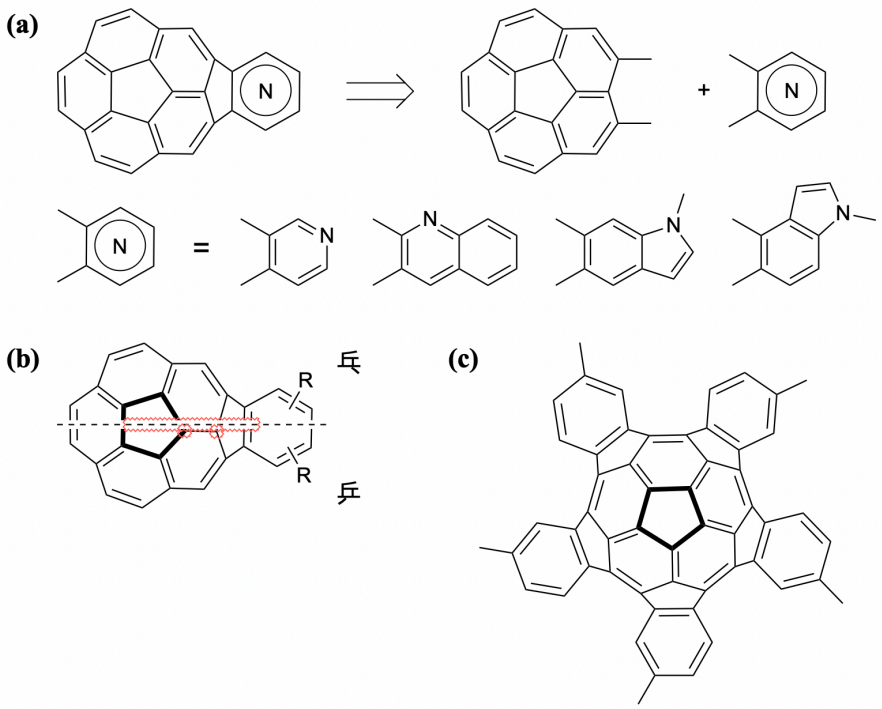

Figure 1. (a) Retrosynthetic analysis of N-heterocyclic indenocorannulene analogs; (b) illustration of 乒 and 乓 configurations with X-indenocorannulenes; (c) example of chiral *sym*-pentaindenocorannulene derivatives.

A robust and facile synthetic strategy for heterocyclic monoindenocorannulene derivatives is achieved via Suzuki-coupling and C-Cl activation (Scheme 1). Pyridine, quinoline, and indole were successfully fused

to corannulene (**1**), rendering four chiral N-heterocyclic monoindenocorannulenes (**4**-**7**). Monoiodocorannulene (**2**) was obtained from **1** by NIS in dichloroethane under the catalysis of $BF_3 \cdot Et_2O$ at gram scale. Subsequent borylation rendered (Bpin)corannulene (**3**) as yellow powders in 72% yield. Precursors **4'**, **5'**, and **6'** were prepared via Suzuki-coupling of **3** with 3-bromo-4-chloropyridine, 3-bromo-2-chloroquinoline, and 5-bromo-6-chloro-*N*-methylindole. Palladium-catalyzed intramolecular arylation of **4'**-**6'** generated four different heterocyclic monoindenocorannulenes, **4**, **5**, **6**, and **7,** in 30%, 31%, 24%, and 8% yields respectively. Compounds **6** and **7**, in an average ratio of 3:1, were separated by preparative HPLC. The physicochemical properties of **4**-**7** were characterized by UV-Vis, fluorescence, CV, and X-ray diffraction.

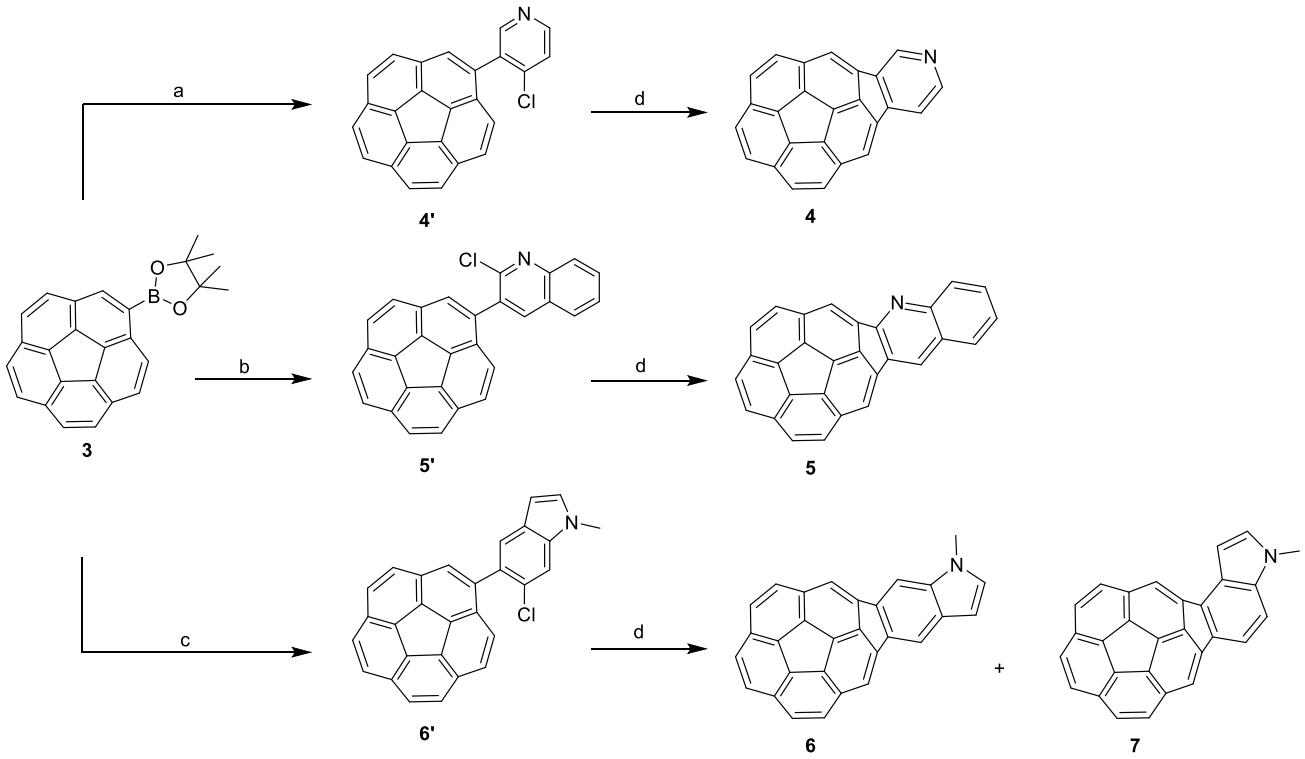

Scheme 1. Synthetic route of heterocyclic monoindenocorannulenes: (a) 3-bromo-4-chloropyridine, $Pd(dppf)Cl_2$, Cs_2CO_3, THF, 95 °C, 1 h, 59%; (b) 3-bromo-2-chloroquinoline, $Pd(dppf)Cl_2$, Cs_2CO_3, THF, 95 °C, 2 h, 73%; (c) 5-bromo-6-chloro-*N*-methylindole, $Pd(dppf)Cl_2$, Cs_2CO_3, THF, 95 °C, 2 h, 82%; (d) $Pd(PCy_3)_2Cl_2$, DBU, DMAc, 170 °C, 3 h, 30% for **4**, 31% for **5**, 24% for **6**, 8% for **7**.

Resolution of Enantiomeric Bowl and Their Absolute Configuration

Because of the slow inversion of indenocorannulene and unsymmetrical nitrogen doping and aromatic ring, **4**-**7** consist of bowl-shaped mirror image conformers. The chiral conformers of **4**-**7** were resolved by HPLC on chiral stationary phases. Specifically, enantiomers of **4** were resolved on Chiralpak®-IC, of **5** on Chiralpak®-IF, and of **6** & **7** on Chiralpak®-IE (Figure 2). Absolute configuration of these chiral bowl-shaped entities cannot be categorized according to "Cahn-Ingold-Prelog" rules. Assignments are archived by the ad hoc 乒 and 乓 characters defined previously.[22] The configurations are assigned by

comparison of experimental and theoretical ECD spectra in the context with a reference 乒 or 乓 structure.

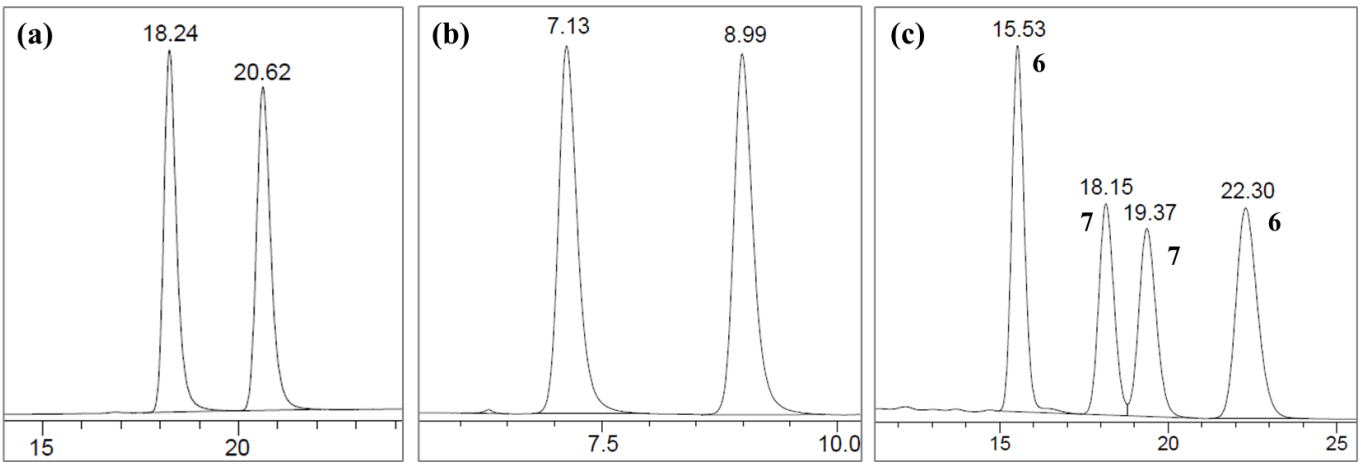

Figure 2. Analytical HPLC chromatograms over chiral phase: (a) **4**, Chiralpak®-IC, heptane/dichloromethane/ isopropanol/triethylamine; (b) **5**, Chiralpak®-IF, hexane/dichloromethane; (c) **6** and **7**, Chiralpak®-IE, hexane/isopropanol; retention times in minutes.

Electronic circular dichroism (ECD) spectra display symmetrical peaks for a pair of enantiomers. By comparing the fit of the experimental data for each enantiomer with computed data for a single reference enantiomer, the absolution configuration can be assigned. The reliability of this method increases with the number of experimental transitions in agreement with computed ones.[22] ECD spectra of enantiomers of **4**-**7** were measured in acetonitrile (Figure 3). Theoretical ECD results, used as reference, are computed at

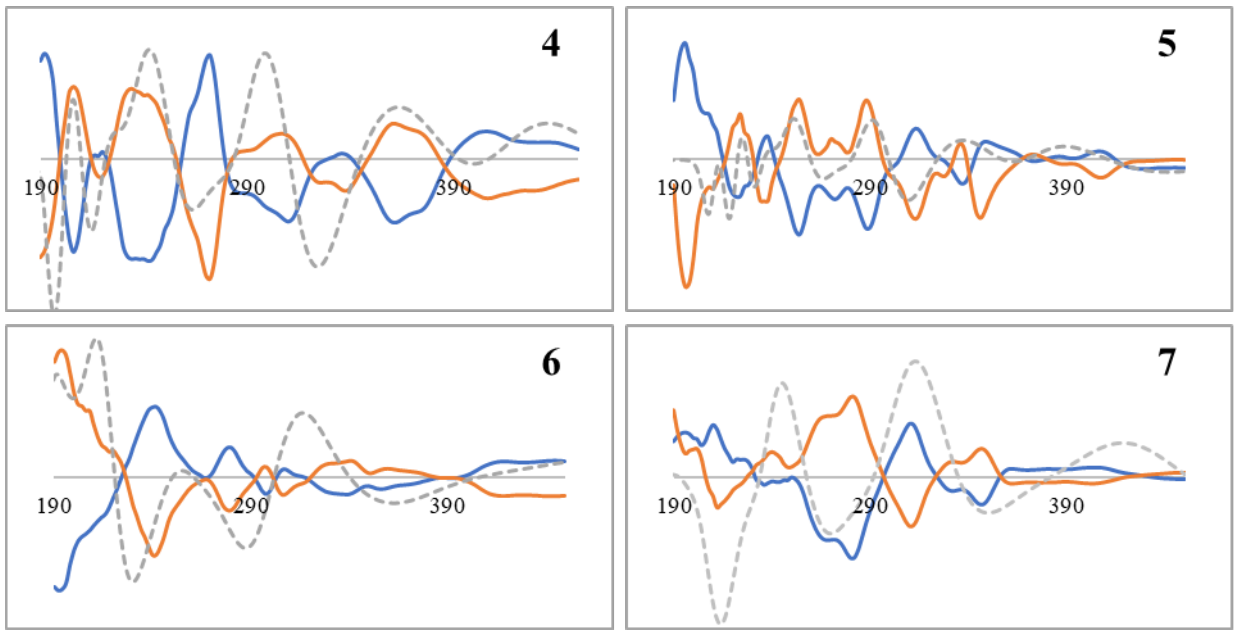

Figure 3. TD-B97-D2/def2-TZVPP//B97-D2/def2-TZVPP computed (gray) and experimental (first eluted blue; second eluted orange) ECD spectra from 190 to 450 nm in acetonitrile.

the TD-B97-D2[25]/def2-TZVPP//B97-D2/def2-TZVPP level of theory, using solvent specifications as in the experiment.

Physical Properties: Luminescence and Electrochemistry

Because of the presence of large conjugated surfaces and lone pair electrons, **4**-**7** exhibit complex physicochemical properties (Figure 4, Table 1). Compound **4** has absorption maxima at 311 and 330 nm with excitation maxima at 264 and 332 nm and emission maximum at 560 nm. The absorption spectra of **5**-**7** are generally similar, with primary absorption maxima at ca. (285±10) nm, shoulder peaks at ca. (340±10) nm, and a second absorption maxima at ca. (347±10) nm. The major emission peaks of **5** and **6** are followed by a shoulder peak respectively. The emission spectrum of **7** displays a shoulder peak before the main peak.

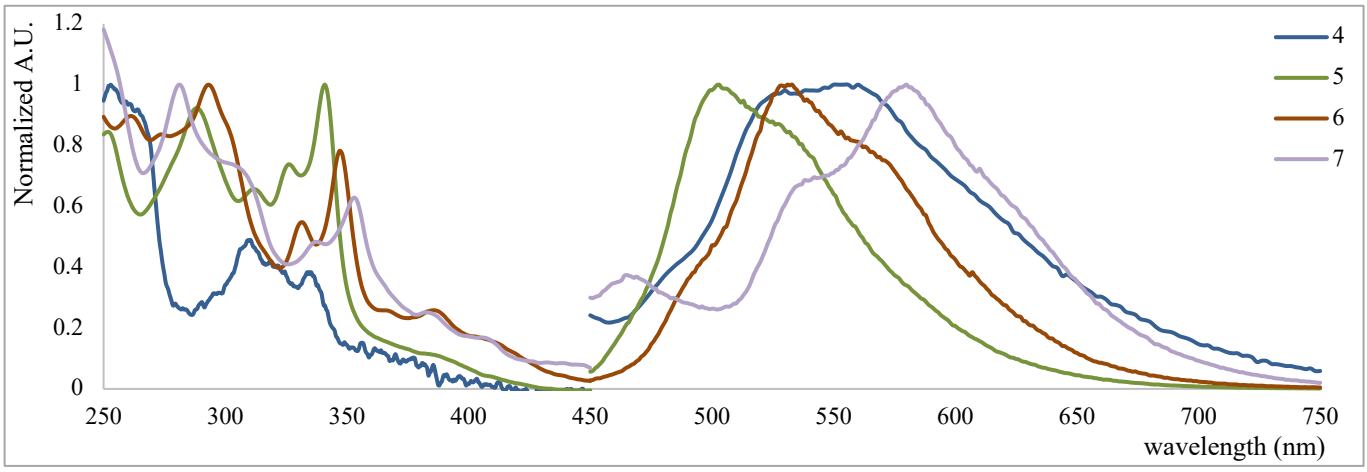

Figure 4. Absorption and emission spectra in cyclohexane (200 μM), excitation wavelengths of **4**-**7** were 331, 341, 347, and 353 nm respectively.

Table 1. Photophysical properties in cyclohexane

Compd.	λ_{abs} (nm)	λ_{em} (nm)	λ_{ex} (nm)
4	311, 330	560	264, 332
5	288, 312, 326, 342	503	341
6	261, 293, 332, 347	531	335, 347
7	281, 353	580	308, 353

Compounds **4**-**7** are subjected to protonation due to the presence of nitrogen. In neutral and acidic environments, the absorption and emission spectra differ slightly (Figure 5). Protonation causes the maximal absorption peaks **4** and **5** to redshift, and the emission maxima to increase by 30-50 nm. The primary absorption maxima of **6** and **7** shift from approximately 280 nm to approximately 300 nm, while

the second absorption maxima at around 350 nm undergo minor shifts to the shorter wavelength. A new shoulder peak in the emission spectra of **6** and **7** appears at about 470 nm after protonation.

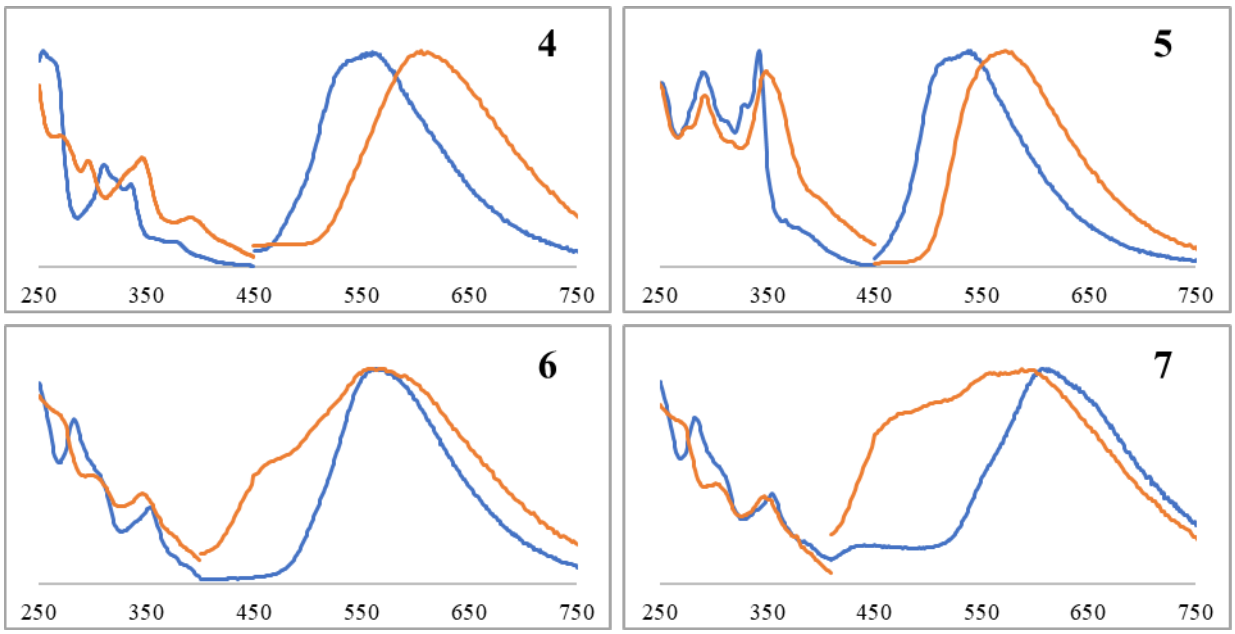

Figure 5. Absorbance and emission spectra in neutral (blue) and HOTf acidified (orange) dichloromethane, wavelength in nanometer.

The cyclic voltammograms of **4**-**7** were collected. First reduction potentials of **4**-**7** were -1.88 V, -1.69 V, -2.20 V, and -2.23 V respectively (Table 2). The addition of an extra aromatic ring generally lowers the reduction potential, and the introduction of an electron-rich group, such as indole, raises the energy required for reduction. Compounds **4** and **5** display semi-reversibility with half-wave potentials of -1.83 V and -1.55 V. Two indole-annulated indenocorannulenes, **6** and **7**, have irreversible voltammograms.

Table 2. Electrochemical properties obtained from cyclic voltammetry

Compd.	E_c (V)	$E_{1/2}$ (V)	I_{pa}/I_{pc}
4	-1.88	-1.83	0.53
5	-1.69	-1.55	0.39
6	-2.20	/	/
7	-2.23	/	/

CONCLUSIONS

A small set of N-heterocyclic curved PAHs have been prepared by a modular Pd-coupling/annulation strategy. These compounds adopt chiral bowl conformations that interconvert on a time scale so slow that resolution of the individual enantiomeric bowl conformers is possible by elution over chiral stationary

phase. Configurational stability is sufficient at room temperature for these to be stored for weeks without noticeable loss of enantiopurity. As such, solution measurement of the ECD spectrum of each enantiomer could be compared to reference quantum mechanical computed spectra and absolute configurations assigned. The physical properties reflect well the expected modification compared to the PAH parent structures and support the idea that these compounds could serve as lead scaffolds for further molecular design and chemical synthesis of biologically and materials active compounds.

EXPERIMENTAL

Crystal Structure Analysis

After gradual evaporation, single crystals of **4** and **7**, appropriate for X-ray diffraction investigation, were selected from saturated solutions of dichloromethane/hexane and dichloromethane respectively. Crystals of **4** stack into the columnar structure through bowl-in-bowl packing (Figure 6a). By directing the five-membered ring into the corannulene core, **7** generates dimers, which aggregate into columnar assembly (Figure 6b).

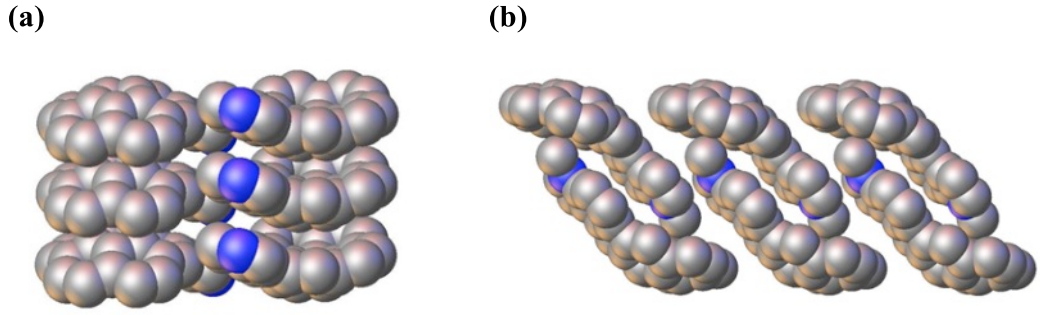

Figure 6. Crystal packing pattern: (a) packing motif of **4**; (b) packing motif of **7**

Computational Methods

The structural and energetic analyses of the molecular systems for all compounds described in this study were carried out with the B97-D2 dispersion enabled density functional method,[26,27] using an ultrafine grid, together with the def2-TZVPP basis set.[28] This basis set can be found in the basis set exchange along with a large number of others, and many have been implemented into our GAMESS program.[29] Full geometry optimizations were performed and uniquely characterized via second derivatives (Hessian) analysis to establish stationary points and effects of zero point and thermal energy contributions. Absorption energies were computed in acetonitrile at the TD-B97-D2[25]/def2-TZVPP//B97-D2/def2-TZVPP level of theory, using solvent specifications as in experiment. From the TD-DFT results, spectra were simulated from the excitation energies and rotation lengths by overlapping Gaussian functions for each transition. Effects of solvent employed the COSMO: *ab initio* continuum method[30,31] using a

dielectric as in experiment, and radii of Klamt.[32] Visualization and analysis of structural and property results were obtained using Avogadro[33] and GaussView (for spectra).[34] Our group develops GAMESS and has also contributed to Gaussian[35] software packages, in this work the G09 ES64L-G09RevE.01 version of the latter was used.

SUPPORTING INFORMATION

Supplementary (synthetic procedures, HPLC conditions and chromatograms, ^{1}H- and ^{13}C-NMR, etc.) data associated with this article can be found, in the online version, at URL: https://www.heterocycles.jp/newlibrary/downloads/PDFsi/27627/105/1.

ACKNOWLEDGEMENTS

We thank the National Basic Research Program of China (2015CB856500) for the support of this work. We appreciate Gao Yan and Dr. Zhang Xiangyang from the instrument center of the School of Pharmaceutical Science and Technology in Tianjin University for the assistance of HRMS analysis. Guo Tianjian is acknowledged for help in ECD, UV-Vis spectrometer, and fluorophotometer.

REFERENCES

1. J. Jampilek, *Molecules*, 2019, **24**, 3839.
2. M. Nakamura, A. Bhatnagar, and J. Sadoshima, *Circ. Res.*, 2012, **111**, 604.
3. S. Kumar, S. Bawa, and H. Gupta, *Mini-Rev. Med. Chem.*, 2009, **9**, 1648.
4. R. Musiol, M. Serda, S. Hensel-Bielowka, and J. Polanski, *Curr. Med. Chem.*, 2010, **17**, 1960.
5. A. J. Kochanowska-Karamyan and M. T. Hamann, *Chem. Rev.*, 2010, **110**, 4489.
6. V. Sharma, P. Kumar, and D. Pathak, *J. Heterocycl. Chem.*, 2010, **47**, 491.
7. N. K. Kaushik, N. Kaushik, P. Attri, N. Kumar, C. H. Kim, A. K. Verma, and E. H. Choi, *Molecules*, 2013, **18**, 6620.
8. C. A. Lipinski, F. Lombardo, B. W. Dominy, and P. J. Feeney, *Adv. Drug Deliv. Rev.*, 1997, **23**, 3.
9. A. Ecker, D. Levorse, D. Victor, and M. Mitcheltree, *ChemRxiv*, 2022, Doi:10.26434/chemrxiv-2022-0835v.
10. S. Ito, Y. Tokimaru, and K. Nozaki, *Angew. Chem. Int. Ed.*, 2015, **54**, 7256.
11. H. Yokoi, Y. Hiraoka, S. Hiroto, D. Sakamaki, S. Seki, and H. Shinokubo, *Nat. Commun.*, 2015, **6**, 8215.
12. Y. Tokimaru, S. Ito, and K. Nozaki, *Angew. Chem.*, 2018, **130**, 9966.
13. T. Nagano, K. Nakamura, Y. Tokimaru, S. Ito, D. Miyajima, T. Aida, and K. Nozaki, *Chem. Eur. J.*, 2018, **24**, 14075.
14. H. Yokoi, S. Hiroto, D. Sakamaki, S. Seki, and H. Shinokubo, *Chem. Sci.*, 2018, **9**, 819.

15. K. Imamura, K. Takimiya, T. Otsubo, and Y. Aso, *Chem. Commun.*, 1999, 1859.
16. M. Saito, T. Tanikawa, T. Tajima, J. D. Guo, and S. Nagase, *Tetrahedron Lett.*, 2010, **51**, 672.
17. Q. Tan, S. Higashibayashi, S. Karanjit, and H. Sakurai, *Nat. Commun.*, 2012, **3**, 891.
18. V. Tsefrikas, A. Greene, and L. Scott, *Org. Chem. Front.*, 2017, **4**, 688.
19. X. Tian, L. M. Roch, N. Vanthuyne, J. Xu, K. K. Baldridge, and J. S. Siegel, *Org. Lett.*, 2019, **21**, 3510.
20. X. Tian, S. Chaiworn, J. Xu, N. Vanthuyne, K. K. Baldridge, and J. S. Siegel, *Org. Chem. Front.*, 2021, **8**, 3653.
21. T. J. Seiders, K. K. Baldridge, G. H. Grube, and J. S. Siegel, *J. Am. Chem. Soc.*, 2001, **123**, 517.
22. Y. Wang, O. Allemann, T. S. Balaban, N. Vanthuyne, A. Linden, K. K. Baldridge, and J. S. Siegel, *Angew. Chem. Int. Ed.*, 2018, **57**, 6470.
23. T. Guo, A. Li, J. Xu, K. K. Baldridge, and J. Siegel, *Angew. Chem. Int. Ed.*, 2021, **60**, 25809.
24. K. Kise, S. Ooi, H. Saito, H. Yorimitsu, A. Osuka, and T. Tanaka, *Angew. Chem. Int. Ed.*, 2022, **61**, e202112589.
25. J.-D. Chai and M. Head-Gordon, *Phys. Chem. Chem. Phys.*, 2008, **10**, 6615.
26. S. Grimme, *J. Chem. Phys.*, 2006, **124**, 034108.
27. S. Grimme, *J. Comput. Chem.*, 2006, **27**, 1787.
28. F. Weigend and R. Ahlrichs, *Phys. Chem. Chem. Phys.*, 2005, **7**, 3297.
29. M. W. Schmidt, K. K. Baldridge, J. A. Boatz, S. T. Elbert, M. S. Gordon, J. H. Jensen, S. Koseki, N. Matsunaga, K. A. Nguyen, S. Su, T. L. Windus, M. Dupuis, and J. A. Montgomery Jr, *J. Comput. Chem.*, 1993, **14**, 1347.
30. A. Klamt, *J. Chem. Soc., Perkin Trans.*, 1993, **2**, 79.
31. K. Baldridge and A. Klamt, *J. Chem. Phys.*, 1997, **106**, 6622.
32. A. Klamt, V. Jonas, T. Bürger, and J. C. Lohrenz, *J. Phys. Chem. A*, 1998, **102**, 5074.
33. M. D. Hanwell, D. E. Curtis, D. C. Lonie, T. Vandermeersch, E. Zurek, and G. R. Hutchison, *J. Cheminform*, 2012, **4**, 17.
34. R. Dennington, T. Keith, and J. Millam, *GaussView, Version 5*, Semichem Inc., 2009.
35. Gaussian09, Version=ES64L-G09 RevE.01, M. J. Frisch, G. W. Trucks, H. B. Schlegel, G. E. Scuseria, M. A. Robb, J. R. Cheeseman, G. Scalmani, V. Barone, B. Mennucci, G. A. Petersson, H. Nakatsuji, M. Caricato, X. Li, H. P. Hratchian, A. F. Izmaylov, J. Bloino, G. Zheng, J. L. Sonnenberg, M. Hada, M. Ehara, K. Toyota, R. Fukuda, J, Hasegawa, M. Ishida, T. Nakajima, Y. Honda, G. Kitao, H. Nakai, T. Vreven, J. A. Montgomery Jr., J. E. PeraIta, F. Ogliaro, M. Bearpark, J. J. Hayd, E. Brothers, K. N. Kudin, V. N. Staroverov, T. Keith, R. Kobayashi, J. Normand, K. Raghavarchari, A. Rendell, J. C. Burant, S. S. Iyengar, J. Tomasi, M. Cossi, N. Rega, J. M. Millam,

M. Klene, J. E. Knox, J. B. Cross, V. Bakken, C. Adamo, J. Jeramillo, R. Gomperts, R. E. Stratmann, O. Yazyev, A. J. Austin, R. Cammi, C. Pomelli, J. W. Ochterski, R. L. Martin, K. Morokuma, V. G. Zakrzewski, G. A. Voth, P. Salvador, J. J. Dannenberg, S. Dapprich, A. D. Daniels, O. Farkes, J. B. Forseman, J. V. Ortiz, J. Cioslowski, and D. J. Fox, Gaussian, Inc., Wallingford, CT, 2013.